

## Dual Role of Cdc42 in Spindle Orientation Control of Adherent Cells<sup>∇</sup>

Masaru Mitsushima,<sup>1</sup> Fumiko Toyoshima,<sup>1,2,3\*</sup> and Eisuke Nishida<sup>1</sup>

Department of Cell and Developmental Biology, Graduate School of Biostudies, Kyoto University, Sakyo-ku, Kyoto 606-8502, Japan<sup>1</sup>; PRESTO, Japan Science and Technology Agency, 4-1-8 Honcho Kawaguchi, Saitama, Japan<sup>2</sup>; and Laboratory of Subcellular Biogenesis, Institute for Virus Research, Kyoto University, Shogoin-Kawahara cho, Sakyo-ku, Kyoto 606-8507, Japan<sup>3</sup>

Received 7 November 2008/Returned for modification 11 December 2008/Accepted 25 February 2009

**The spindle orientation is regulated by the interaction of astral microtubules with the cell cortex. We have previously shown that spindles in nonpolarized adherent cells are oriented parallel to the substratum by an actin cytoskeleton- and phosphatidylinositol 3,4,5-triphosphate [PtdIns(3,4,5)P3]-dependent mechanism. Here, we show that Cdc42, a Rho family of small GTPases, has an essential role in this mechanism of spindle orientation by regulating both the actin cytoskeleton and PtdIns(3,4,5)P3. Knockdown of Cdc42 suppresses PI(3)K activity in M phase and induces spindle misorientation. Moreover, knockdown of Cdc42 disrupts the cortical actin structures in metaphase cells. Our results show that p21-activated kinase 2 (PAK2), a target of Cdc42 and/or Rac1, plays a key role in regulating actin reorganization and spindle orientation downstream from Cdc42. Surprisingly, PAK2 regulates spindle orientation in a kinase activity-independent manner. βPix, a guanine nucleotide exchange factor for Rac1 and Cdc42, is shown to mediate this kinase-independent function of PAK2. This study thus demonstrates that spindle orientation in adherent cells is regulated by two distinct pathways downstream from Cdc42 and uncovers a novel role of the Cdc42-PAK2-βPix-actin pathway for this mechanism.**

Alignment of the mitotic spindles with a predetermined axis, which confines the plane of cell division, occurs in many types of cells and is crucial for morphogenesis and embryogenesis. Cell geometry (30, 32, 47), cell polarity (6, 24, 35), and cell-cell adhesions (20, 22, 48) are proposed to be the determinants for the axis of the spindles. In most cases, spindle alignment along the predetermined axis requires both astral microtubules and the actin cytoskeleton and is believed to involve dynein-dependent microtubule pulling forces functioning at the cell cortex (4, 12, 31).

We have previously shown that in nonpolarized adherent cells, such as HeLa cells, integrin-mediated cell-substrate adhesion orients the spindles parallel to the substratum, which ensures that both daughter cells remain attached to the substrate after cell division (42). This mechanism requires the actin cytoskeleton, astral microtubules, the microtubule plus-end-tracking protein EB1, and myosin X. Furthermore, our recent study has shown that the lipid second messenger phosphatidylinositol 3,4,5-triphosphate [PtdIns(3,4,5)P3] is also essential to this mechanism. PtdIns(3,4,5)P3 is accumulated in the midcortex of metaphase cells, which is important for the localized accumulation of dynactin, a dynein-binding partner, at the midcortex. We have proposed that PtdIns(3,4,5)P3 directs dynein/dynactin-dependent pulling forces on the spindle to the midcortex and orients the spindle parallel to the substratum (43). However, the molecular mechanisms that regu-

late the actin cytoskeleton and PtdIns(3,4,5)P3 in the spindle orientation control remain unknown.

The Rho family of GTPases, including Rho, Rac, and Cdc42, plays central roles in the regulation of not only the actin cytoskeleton but also microtubules in the control of various activities of cell motility, including cell adhesion, cell migration, and cell cycle progression (9, 33, 41). Rho family GTPases are also reported to regulate several mitotic events. RhoA plays a crucial role in contractile ring function and localizes to the cleavage furrow along with its effectors, ROCK, citron kinase, and mDia, during cytokinesis (18, 11). Cdc42 and its effector, mDia3, are reported to regulate the alignment of chromosomes during prometaphase and metaphase (49). Interestingly, Cdc42 is also required for proper spindle positioning in polarized cells such as budding yeast (*Saccharomyces cerevisiae*), *Caenorhabditis elegans* one-cell stage embryos, and mouse oocytes, which undergo asymmetric cell division (1, 23, 13, 28). However, how Cdc42 regulates spindle orientation and whether it has a role in spindle orientation in nonpolarized cells remain unknown.

Here, we show that Cdc42 is required for the mechanism that orients the spindle parallel to the substratum in nonpolarized adherent cells. Moreover, our results show that Cdc42 regulates both PtdIns(3,4,5)P3 and the actin cytoskeleton through PI(3)K- and p21-activated kinase 2 (PAK2)/βPix-signaling pathways, respectively. Both pathways are required for the localized accumulation of dynein/dynactin complexes in the midcortex in metaphase cells and, thus, for the proper spindle orientation parallel to the substratum.

### MATERIALS AND METHODS

**Antibodies and materials.** The following antibodies were used: anti-PAK1, anti-PAK2, anti-Akt, anti-phospho-Akt (Ser473), anti-phospho-Aurora A (Thr288) (Cell Signaling), and anti-βPix (Upstate) rabbit polyclonal antibodies

\* Corresponding author. Mailing address: Laboratory of Subcellular Biogenesis, Institute for Virus Research, Kyoto University, Shogoin-Kawahara cho, Sakyo-ku, Kyoto 606-8507, Japan. Phone: 81-75-751-4015. Fax: 81-75-751-4016. E-mail: ftoyoshi@virus.kyoto-u.ac.jp.

§ Supplemental material for this article may be found at <http://mcb.asm.org/>.

<sup>∇</sup> Published ahead of print on 9 March 2009.

and anti-RhoA (F-7), anti-cyclin B1, anti-cyclin A2, anti-Myc (9E10) (Santa Cruz), anti-Cdc42, anti-BubR1, anti-Git1, anti-p150<sup>Glued</sup>, anti-Aurora A (BD Transduction), anti-Rac1, anti-cyclin E (Upstate), and anti-green fluorescent protein (GFP) (Clontech) mouse monoclonal antibodies. Horseradish peroxidase-conjugated anti-mouse immunoglobulin G (IgG) or anti-rabbit IgG antibodies were obtained from GE Healthcare. MG132 and LY294002 were obtained from Calbiochem.

**Plasmid constructs.** The full length of human PAK2 was amplified with the KOD Plus polymerase mixture (Toyobo) from the human placenta cDNA library (Clontech) with the following primer pair: 5'-GCAGGATCCATGTC TGATAACGGAGAAGCTG and 5'-GGCGGATCCTTAACGGTTACTCTT CATTGC. The amplified products were digested by BamHI and subcloned into pEGFP-C1 (Clontech). The sequence was confirmed by DNA sequencing. The mutant constructs (PAK2-res, PAK2-res-K278R, and PAK2-res-H82, 85L) were created by two-step PCR methods using the following complemented primers (the sequences of the forward primers are shown): PAK2-res, 5'-CAGCCAAAGAAGGAGTTAATTATCAACGAGATTCTGGTG; PAK2-res-K278R, 5'-GGAGGTTGCTATCAGACAAATTAATTTAC; PAK2-res-H82, 85L, 5'-CCATCTGATTTTGACTCACCCTGTTGGCTTGTGATGCT; and PAK2-res-P185R186A, 5'-CCTCCCGTTATTGCCGCGGCACCGGATCATA CGAAA. For the first step, the N-terminal and C-terminal fragments of each PAK2 mutant were amplified with a 5' primer paired with each reverse primer and with a 3' primer paired with each forward primer. For the second step, the full length of each PAK2 mutant was amplified with 5' primers and 3' primers, using the first PCR products as a template. The amplified products were subcloned into pEGFP-C1 and pcDL-SR $\alpha$ -Myc, and the mutations were confirmed by DNA sequencing. pCS2-Myc- $\beta$ Pix was kindly provided by H. Sugimura.

**Cell culture, synchronization, and transfection.** HeLa cells were cultured in Dulbecco modified Eagle medium with 10% fetal bovine calf serum. To synchronize cells in M phase, HeLa cells were arrested at the G<sub>1</sub>/S boundary by a double thymidine block, released from the arrest by being washed with fresh medium, and incubated for 10 h. In all experiments, HeLa cells were plated on fibronectin-coated coverslips (BD BioCoat). The plasmids were transfected into HeLa cells with Lipofectamine Plus (Invitrogen) 8 h after the release from the first thymidine block and incubated for 1 h. Immediately after the removal of the transfection complexes by washing with fresh medium, thymidine was added and incubated for 15 h. Cells were fixed 10 h after the release from the second thymidine block.

**Spindle orientation analysis.** Spindle orientation analysis was described previously (42). Briefly, z-stack images were taken from 0.5- $\mu$ m-thick sections of metaphase cells that were immunostained with anti- $\gamma$ -tubulin and anti- $\alpha$ -tubulin (T5192 and T6199, respectively; Sigma) antibodies and Hoechst (Sigma), and the linear distance and the vertical distance between the two poles of the metaphase spindles were measured. Then, the spindle angle was calculated by inverse trigonometric function. Fifty metaphase cells with normally aligned chromosomes were analyzed in each condition.

**Cell staining, image analysis, and time lapse.** Synchronized HeLa cells in M phase were fixed for 5 min with methanol at  $-20^{\circ}\text{C}$ , washed three times with phosphate-buffered saline (PBS), blocked with 3% bovine serum albumin in PBS, and incubated with the primary antibodies overnight at  $4^{\circ}\text{C}$ , followed by incubation with the secondary antibody (Alexa Fluor 488- or Alexa Fluor 546-conjugated goat anti-rabbit or -mouse IgG antibodies; Molecular Probes) for 1 h at room temperature. For  $\gamma$ -tubulin staining, cells were fixed for 5 min with 3.7% formaldehyde at  $37^{\circ}\text{C}$ , followed by incubation for 20 min with methanol at  $-20^{\circ}\text{C}$ . For dynactin p150<sup>Glued</sup> staining, cells were preextracted with 0.5% Triton X-100 in PHEM buffer (60 mM PIPES [piperazine-*N,N'*-bis(2-ethanesulfonic acid)], 25 mM HEPES, 10 mM EGTA, and 4 mM MgSO<sub>4</sub>) with 5  $\mu$ M taxol for 1 min and fixed with methanol at  $-20^{\circ}\text{C}$  for 5 min. Phalloidin staining was performed as described previously (27). Briefly, cells were fixed for 1 min with 2% glutaraldehyde/300 mM sucrose in PBS at room temperature, permeabilized for 3 min with 1% glutaraldehyde/0.5% Triton X-100 in PBS at room temperature, washed three times with PBS, and quenched for 5 min with 1.5 mg/ml glycine in PBS at room temperature, followed by being washed with PBS three times, blocked with 3% bovine serum albumin in PBS, and incubated with Oregon Green-conjugated phalloidin (Molecular Probes). Deconvolved images were taken by using DeltaVision optical sectioning systems with softWoRx software. Confocal images were acquired by using a confocal laser scanning microscope (Radiance 2100; Bio-Rad). For live imaging, we used a DeltaVision optical sectioning system with a temperature-controlled and motorized stage. During the acquisition of the time-lapse images, cells were grown in the medium with 20 mM HEPES (pH 7.3) in plastic-bottom chambers (Integrated BioDiagnostics) coated with human fibronectin (F0895; Sigma). During the acquisition of the time-lapse images, HeLa cells expressing GFP-H2B were synchronized in M phase by

releasing them from a double thymidine block. Time-lapse images were obtained every 5 min. All images were taken in the same exposure time.

**Lipid delivery.** The phosphoinositide-histone complexes were delivered to the cells as previously described (43), with some modifications. In the previous study, we used the PtdIns(3,4,5)P<sub>3</sub>-histone complexes (final concentration, 150  $\mu$ M PIP3-50  $\mu$ M histone), which were prepared by incubating 300  $\mu$ M long-chain (Di-C<sub>16</sub>) PtdIns(3,4,5)P<sub>3</sub> (10  $\mu$ l) (Echelon) with 100  $\mu$ M histone (10  $\mu$ l) (Echelon) (43). We have found that the PtdIns(3,4,5)P<sub>3</sub>-histone complex (final concentration, 100  $\mu$ M PIP3-50  $\mu$ M histone) induces the activation of PI(3)K more efficiently (see Fig. S1 in the supplemental material). Thus, in the present study, we used the latter complexes. The complexes were vortexed vigorously and incubated for 5 min at room temperature, diluted with culture medium (80  $\mu$ l), added to the cells, and incubated for 5 or 10 min in a temperature-controlled CO<sub>2</sub> incubator.

**siRNAs and rescue experiments.** The small interfering RNAs (siRNAs) of human RhoA, Cdc42, Rac1, PAK1, PAK2,  $\beta$ 1 integrin,  $\beta$ Pix, and Git1 were designed as described previously (2, 5, 7, 10, 14). Single-strand RNA was synthesized by Japan Bio Service. Sense and antisense siRNAs were annealed according to the manufacturer's instructions. HeLa cells were transfected with the annealed siRNAs by Oligofectamine (Invitrogen) for 5 h, washed with fresh medium, and subjected to a double thymidine block. The expression levels of each protein were confirmed by immunoblotting using specific antibodies. For PAK2 siRNA rescue experiments, we constructed pEGFP-PAK2-res, which was resistant to PAK2 siRNA, by introducing five silent substitutions in the PAK2 siRNA-target region. HeLa cells were transfected with PAK2 siRNA by using Oligofectamine for 5 h, washed with fresh medium, and subjected to a double thymidine block. Eight hours after the release from the first thymidine block, pEGFP-PAK2-res was transfected into cells with Lipofectamine Plus for 50 min and subjected to the second thymidine block. We selected the GFP-PAK2-res-transfected metaphase cells by observing the intensity of the fluorescence signal of GFP (see Fig. S2 in the supplemental material).

**Immunoprecipitation.** M phase-synchronized HeLa cells were washed with PBS and lysed with the lysis buffer (150 mM NaCl, 2.5 mM KCl, 10 mM Na<sub>2</sub>HPO<sub>4</sub> · 12H<sub>2</sub>O, 1.8 mM KH<sub>2</sub>PO<sub>4</sub>, 1% Triton X-100, 10 mM NaF, 10 mM  $\beta$ -glycerophosphate, 20  $\mu$ g/ml aprotinin, 100  $\mu$ g/ml leupeptin). Cell lysates were incubated overnight with anti-PAK2 antibody or rabbit IgG at  $4^{\circ}\text{C}$  and then incubated with protein A-Sepharose beads (GE Healthcare) for 2 h. The bead complexes were washed three times with the lysis buffer and subjected to immunoblotting with anti- $\beta$ Pix, anti-Git1, or anti-PAK2 antibodies.

## RESULTS

### Cdc42 and Rac1 regulate spindle orientation in HeLa cells.

To examine the potential involvement of the Rho family of GTPases in the spindle orientation control, we downregulated RhoA, Rac1, or Cdc42 proteins by siRNA in synchronized HeLa cells (Fig. 1A). In metaphase, i.e., when the chromosomes were aligned on the metaphase plate, spindles were properly oriented parallel to the substratum in the cells transfected with GFP siRNA or RhoA siRNA but misoriented in the cells transfected with Rac1 siRNA or Cdc42 siRNA (Fig. 1B). The angle between the axis of a metaphase spindle and the substrate surface ( $\alpha^{\circ}$ ) (Fig. 1C, left) was measured in 50 metaphase cells in each condition. The spindle angle fell within  $10^{\circ}$  in more than 75% of the GFP siRNA- or RhoA siRNA-transfected cells but in less than 50% and 25% of the cells transfected with Rac1 siRNA and Cdc42 siRNA, respectively (Fig. 1C, right). The spindles were most severely misoriented in the Cdc42 siRNA-transfected cells (Fig. 1C, right). The average spindle angles were  $6.55^{\circ}$ ,  $4.85^{\circ}$ ,  $12.2^{\circ}$ , and  $21.8^{\circ}$  in the GFP siRNA-, RhoA siRNA-, Rac1 siRNA-, Cdc42-transfected cells, respectively (Fig. 1C, right). The spindle misorientation in the cells transfected with both Rac1 siRNA and Cdc42 siRNA was similar to that in the cells transfected with Cdc42 siRNA alone but was more severe than that in the cells transfected with Rac1 siRNA alone (Fig. 1C). It has been reported that Cdc42 is required for microtubule attachment to kineto-

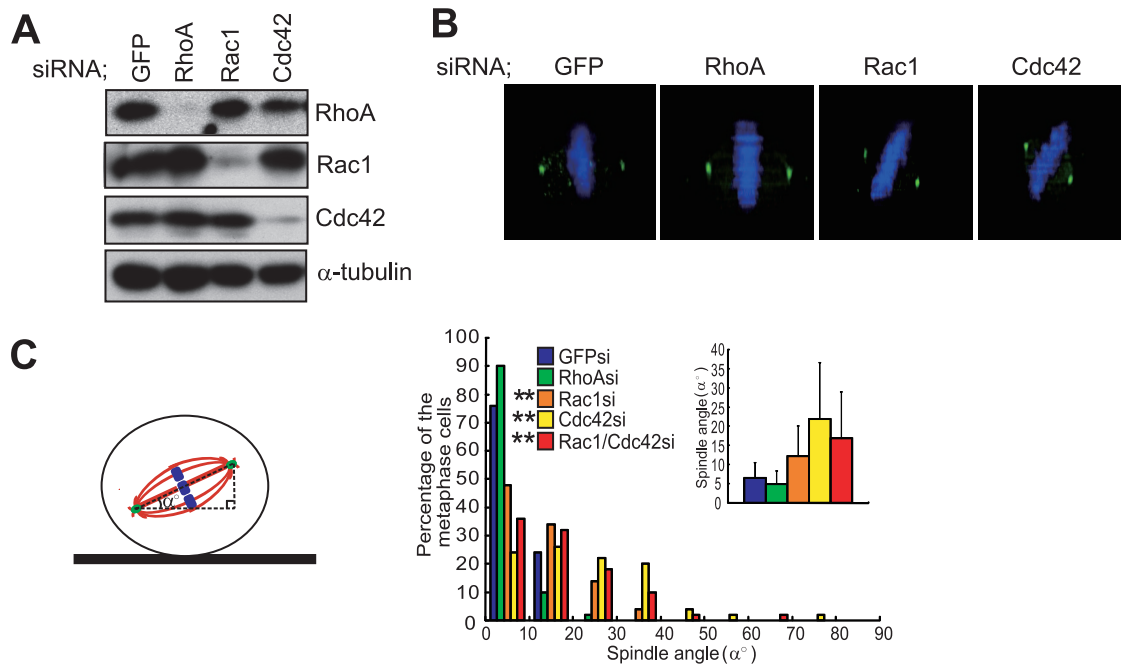


FIG. 1. Cdc42 and Rac1 are required for the spindle orientation parallel to the substratum in HeLa cells. (A) Total lysates of M phase-synchronized HeLa cells transfected with GFP siRNA, RhoA siRNA, Rac1 siRNA, or Cdc42 siRNA were subjected to immunoblotting with anti-RhoA, anti-Rac1, anti-Cdc42, and anti- $\alpha$ -tubulin antibodies. (B) The *X-Z* projections of metaphase cells as prepared in panel A and stained with anti- $\gamma$ -tubulin (green) and Hoechst (blue). (C) The spindle angle (left;  $\alpha^\circ$ ) was measured in metaphase cells. Distribution (right; histogram;  $n = 50$ ) and the average (right; inset; mean  $\pm$  standard deviation;  $n = 50$ ) of spindle angles in each condition are shown (right). \*\*,  $P$  value of  $<0.001$  compared with that of control GFP siRNA, analyzed by F-test.

chores during mitosis (49). Consistent with this report, depletion of Cdc42 led to an increase in the number of cells with misaligned chromosomes to about 10% of the cells (see Fig. S3 in the supplemental material). Thus, about 90% of metaphase cells have normally aligned chromosomes. Similarly, more than 85% of the misoriented spindles in the Cdc42 siRNA-transfected cells seem to have normally aligned chromosomes (see siCdc42 at the bottom of Fig. S3 in the supplemental material). To examine in more detail the integrity of microtubule attachment to kinetochores in the misoriented spindles, in which chromosomes seem to be aligned normally, localization of BubR1 was investigated. BubR1 is known to localize to kinetochores, which are unattached to microtubules, and dissociate from kinetochores at metaphase when microtubules attach to kinetochores (16). In the Rac1 siRNA- and Cdc42 siRNA-transfected cells, BubR1 localized to the kinetochores during prometaphase (see Rac1si and Cdc42si in Fig. S4 in the supplemental material), and its kinetochore localization was lost at metaphase, even when the spindle was misoriented (see Rac1si and Cdc42si in Fig. S4 in the supplemental material). This behavior of BubR1 is normal, indicating that microtubule attachment to kinetochores in the misoriented spindles observed in the Rac1 siRNA- and Cdc42 siRNA-transfected cells is intact. The Rac1 siRNA- and Cdc42 siRNA-transfected cells were also able to separate their chromosomes along the axis of their spindles, even when the spindle axis was tilted to the substrate plane (see Movies S2 and S3 in the supplemental material). This clearly demonstrates that the misoriented spindles in the Rac1 siRNA- and Cdc42 siRNA-transfected cells are functionally intact. We also examined the effects of the

dominant-negative mutant of Cdc42 on the spindle orientation. Consistent with the previous report (49), expression of the dominant-negative Cdc42N17 mutant in synchronized HeLa cells led to an increase in the number of the cells with misaligned chromosomes (data not shown). We found that expression of Cdc42N17, but not a control vector, also caused severe spindle misorientation in metaphase cells with normally aligned chromosomes (see Fig. S5 in the supplemental material). These results, taken together, demonstrate that Cdc42 and Rac1 are required for the proper spindle orientation parallel to the substratum.

**Cdc42 is required for the activation of PI(3)K during mitosis.** We have recently shown that PI(3)K is activated during M phase in a  $\beta 1$  integrin-dependent manner and that PtdIns(3,4,5)P<sub>3</sub>, a lipid product of PI(3)K, is accumulated in the midcortex of metaphase cells, which is required for the proper spindle orientation parallel to the substratum (43). To investigate whether Rho family GTPases are involved in the activation of PI(3)K, we examined the endogenous PI(3)K activity in synchronized cells. In the control GFP siRNA-transfected cells, the endogenous PI(3)K activity, which can be monitored by the phosphorylation state of Akt, was slightly increased in S phase (GFP and phospho-Akt, 6 h) (Fig. 2B), and the activated activity was maintained during M phase (GFP and phospho-Akt, 10 h and 12 h) (Fig. 2B), as reported previously (34, 40, 43). While the endogenous PI(3)K activity was unchanged in M phase-synchronized cells transfected with RhoA siRNA or Rac1 siRNA (RhoA and Rac1) (Fig. 2A), it was suppressed significantly in the Cdc42 siRNA-transfected cells (Cdc42) (Fig. 2A and B) and in the cells transfected with

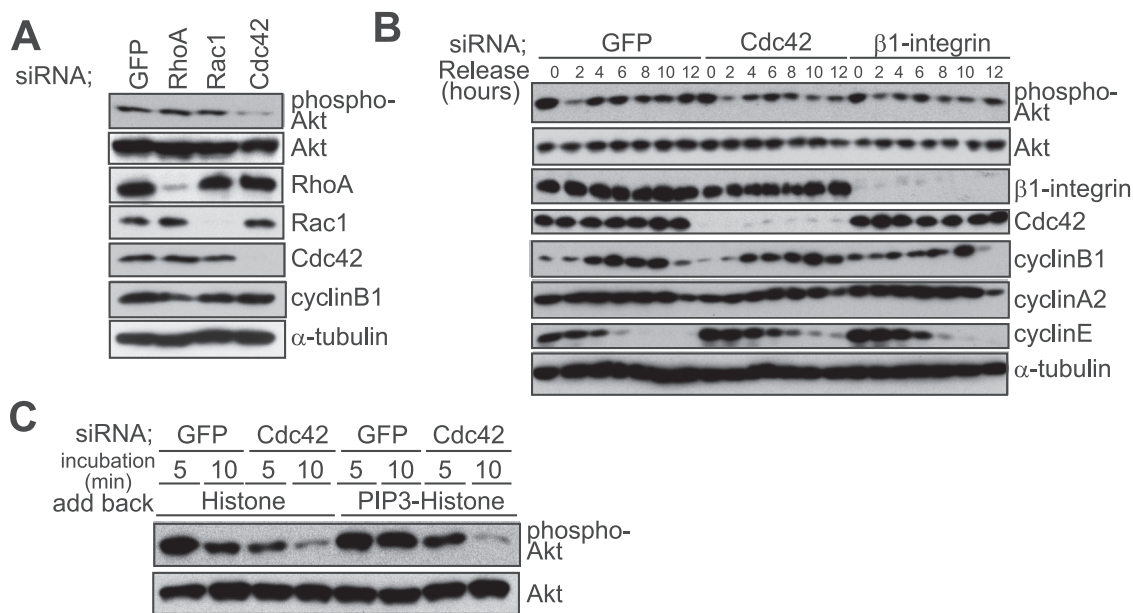


FIG. 2. Cdc42 is required for the activation of PI(3)K during mitosis. (A) Total lysates of M phase-synchronized HeLa cells transfected with GFP siRNA, RhoA siRNA, Rac1 siRNA, or Cdc42 siRNA were subjected to immunoblotting with anti-RhoA, anti-Rac1, anti-Cdc42, anti-phospho-Akt (Ser473), anti-Akt, anti-cyclin B1, and anti- $\alpha$ -tubulin antibodies. (B) Total lysates of synchronized cells transfected with GFP siRNA, Cdc42 siRNA, or  $\beta$ 1 integrin siRNA were subjected to immunoblotting with anti-phospho-Akt (Ser473), anti-Akt, anti-Cdc42, anti- $\beta$ 1 integrin, anti-cyclin B1, anti-cyclin A2, anti-cyclin E, and anti- $\alpha$ -tubulin antibodies. (C) Total lysates of M phase-synchronized cells transfected with GFP siRNA or Cdc42 siRNA, pretreated with LY294002 for 2 h, washed with condition medium, and exposed to carrier histone or PIP3-histone for 5 min or 10 min were subjected to immunoblotting with anti-phospho-Akt (Ser473) and anti-Akt antibodies.

$\beta$ 1 integrin siRNA ( $\beta$ 1 integrin) (Fig. 2B) (43). It should be noted that the cell cycle progression, which was monitored by the expression profiles of cyclin B1, cyclin A2, and cyclin E, was normal for the cells transfected with Cdc42 siRNA or  $\beta$ 1 integrin siRNA (Fig. 2B).

We have previously shown that the introduction of exogenous PtdIns(3,4,5)P3 to the PI(3)K-inhibited cells restores the midcortical accumulation of PtdIns(3,4,5)P3 in metaphase cells and induces proper spindle orientation within 10 min after being delivered (43). To test whether Cdc42 plays a role in this mechanism, we examined endogenous PI(3)K activity in the M phase-synchronized cells that were pretreated with the PI(3)K inhibitor LY294002 and exposed to PtdIns(3,4,5)P3-histone complexes. Because a positive feedback loop, which requires endogenous PI(3)K activity, has been previously demonstrated to play a role in establishing the midcortical accumulation of PtdIns(3,4,5)P3 in metaphase cells (43), we replaced the medium that contains LY294002 with a condition medium that does not contain LY294002 immediately before delivering the PtdIns(3,4,5)P3-histone complexes to the cells. In the control GFP siRNA-transfected cells exposed to a carrier histone, endogenous PI(3)K activity was increased within 5 min but decreased rapidly within 10 min after delivering (histone and GFP) (Fig. 2C), whereas it was sustained during the 10 min after delivering in the GFP siRNA-transfected cells exposed to PtdIns(3,4,5)P3 (PIP3-histone and GFP) (Fig. 2C). In the Cdc42 siRNA-transfected cells, the activation of endogenous PI(3)K activity was significantly reduced, and the activated activity was decreased rapidly within 10 min, even in the cells exposed to PtdIns(3,4,5)P3 (PIP3-histone and Cdc42) (Fig. 2C). These results indicate that Cdc42 is required for the

activation of endogenous PI(3)K induced by exogenously added PtdIns(3,4,5)P3.

**A Cdc42/Rac1-PAK2 module regulates actin reorganization during mitosis.** During mitosis, HeLa cells reorganize their actin cytoskeletons drastically and round up. In metaphase cells, cortical actins line the plasma membrane throughout the cortex, and retraction fibers, composed of fibrous actin filaments, maintain the cell-substrate adhesions (GFP) (Fig. 3A). Our previous result indicating that disruption of the actin cytoskeleton by latrunculin B, an inhibitor of actin polymerization, causes spindle misorientation has shown the requirement of the actin cytoskeleton in the spindle orientation control of adherent cells (42). In RhoA siRNA-transfected cells, retraction fibers were still observed, although cell rounding was slightly inhibited (RhoA) (Fig. 3A; see also Fig. S6 in the supplemental material), as previously described in the cells treated with the RhoA inhibitor C3 toxin or the ROCK inhibitor Y27632 (25). In contrast, in Rac1 siRNA-transfected cells, retraction fibers were severely disrupted, and cortical actin was also disrupted (Rac1) (Fig. 3A). Cortical actin structures were severely disrupted, and the number of retraction fibers was reduced in the Cdc42 siRNA-transfected cells (Cdc42) (Fig. 3A; see also siCdc42 in Fig. S7 in the supplemental material). We have previously shown that these actin structures were essentially normal in the PI(3)K-inhibited cells (43). These results suggest that Cdc42 and Rac1 regulate actin reorganization during mitosis through a pathway that is distinct from the PI(3)K pathway and that both pathways are required for the proper spindle orientation parallel to the substratum in adherent cells.

PAK is a well-known effector of Cdc42 and Rac1 and regulates

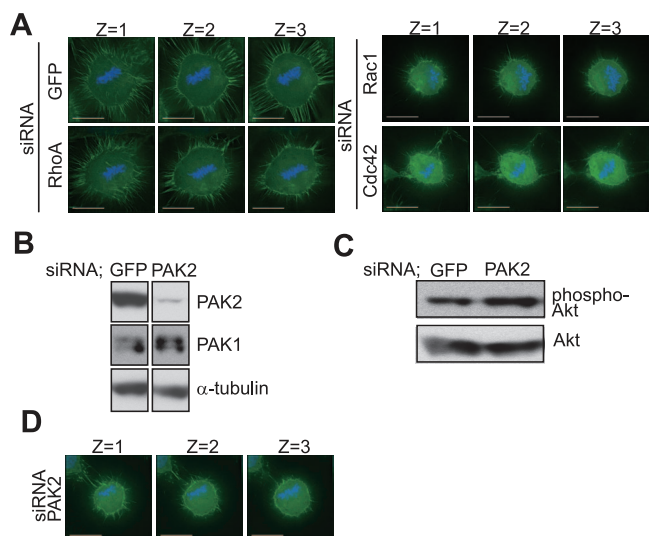


FIG. 3. Cdc42 and PAK2 regulate actin reorganization during mitosis. (A) Z-stack images ( $2.5 \mu\text{m}$  apart) with phalloidin (green) and Hoechst (blue) in metaphase HeLa cells transfected with GFP siRNA, RhoA siRNA, Rac1 siRNA, or Cdc42 siRNA. The scale bar represents  $10 \mu\text{m}$ . (B) Total lysates of M phase-synchronized cells transfected with GFP siRNA or PAK2 siRNA were subjected to immunoblotting with anti-PAK2, anti-PAK1, and anti- $\alpha$ -tubulin antibodies. (C) Total lysates of M phase-synchronized HeLa cells transfected with GFP siRNA or PAK2 siRNA were subjected to immunoblotting with anti-phospho-Akt (Ser473) and anti-Akt antibodies. (D) Z-stack images ( $2.5 \mu\text{m}$  apart) with phalloidin (green) and Hoechst (blue) in metaphase cells transfected with PAK2 siRNA. The scale bar represents  $10 \mu\text{m}$ .

the actin cytoskeleton in various cell motilities (3, 38). To examine the possible role for PAK in actin reorganization during mitosis, we depleted the PAK2 protein specifically with siRNA in synchronized HeLa cells (Fig. 3B). The endogenous PI(3)K activity in M phase-synchronized cells was not significantly changed in the PAK2 siRNA-transfected cells (Fig. 3C). However, the cortical actin structures were slightly disrupted, and retraction fibers were reduced in the PAK2 siRNA-transfected cells (Fig. 3D; see also Fig. S7 in the supplemental material). These results suggest that PAK2 functions downstream from Cdc42 and regulates actin reorganization through a pathway that is distinct from the PI(3)K-PtdIns(3,4,5)P3 pathway.

**PAK2 regulates spindle orientation.** We next examined whether PAK2 is required for the proper spindle orientation. In the control GFP siRNA-transfected cells, the spindles were properly oriented parallel to the substratum (GFP) (Fig. 4A and B). In the PAK2 siRNA-transfected cells, however, the spindles were severely misoriented (PAK2) (Fig. 4A and B). The behavior of BubR1 and the spindle formation were normal in the PAK2 siRNA-transfected cells, indicating that the assembly of misoriented spindles in the PAK2 siRNA-transfected cells is intact (see Fig. S4, PAK2si, and Fig. S8 in the supplemental material). To confirm that the effect of PAK2 siRNA on spindle orientation results from the knockdown of the PAK2 protein, rather than unspecific effects of the used RNA duplexes, we transfected with a rescue construct (GFP-PAK2-res) which encodes a GFP fusion of PAK2 and is resistant to the siRNA due to silent substitutions of the siRNA target region into PAK2-depleted cells (Fig. 4C and D). Ex-

pression of GFP-PAK2-res, but not GFP alone, restored the proper spindle orientation in the PAK2 siRNA-transfected cells (Fig. 4D), confirming the requirement of PAK2 for proper spindle orientation. The time-lapse images of GFP-H2B expressing HeLa cells that were transfected with PAK2 siRNA show that one of the two daughter cells with misoriented spindles fails to maintain connection to the substratum after cell division (see Movie S4 in the supplemental material). A similar phenotype was observed in the cells transfected with Cdc42 siRNA (see Movie S3 in the supplemental material), in which spindles were misoriented. These results demonstrate that both Cdc42 and PAK2 are necessary for the proper spindle orientation parallel to the substrate plane, which ensures that both daughter cells remain attached to the substratum after cell division. To test whether the PAK2-dependent mechanism for spindle orientation exists in nontransformed cells, we used MCF-10A cells, nontransformed mammary epithelial cells. Knockdown of PAK2 by siRNA also induced severe misorientation of the spindles in MCF-10A cells (see Fig. S9A and B in the supplemental material) and in HeLa cells, suggesting that this mechanism for spindle orientation is functioning in both HeLa cells and nontransformed MCF-10A cells. We also examined the requirement of PAK1 for the proper spindle orientation by knocking it down with siRNA in synchronized HeLa cells (see Fig. S10A in the supplemental material). Depletion of PAK1 also induced severe misorientation of the spindles (see Fig. S10B in the supplemental material) without deteriorating the spindle organization (see PAK1si in Fig. S4 in the supplemental material). The spindles were more severely misoriented in the cells depleted of both PAK1 and PAK2 than in the cells depleted of either of the two (see Fig. S10B in the supplemental material), suggesting that PAK1 and PAK2 regulate spindle orientation either independently or redundantly.

**PAK2 regulates spindle orientation in a Cdc42/Rac1 binding-dependent and kinase activity-independent manner.** PAK is thought to exist as a homodimer in cells, probably in a *trans*-inhibited conformation, where the kinase inhibitory domain of one PAK molecule binds the C-terminal catalytic domain of the other (21). Cdc42 and/or Rac binding to the CRIB domain causes a change in the conformation of the kinase inhibitory domain, which then disrupts its interaction with the catalytic domain (21). We examined whether PAK2 requires the Cdc42 and/or Rac1 binding and sequential conformational change to regulate spindle orientation. To this end, we constructed GFP-PAK2-res-H82, 85L, a GFP fusion of an siRNA-resistant PAK2 mutant, in which His82 and His85 in the CRIB domain were replaced by Leu, and transfected it to the PAK2 siRNA-transfected cells. This mutant form of PAK2 was reported to be unable to interact with Cdc42 or Rac1 (37). GFP-PAK2-res-H82, 85L was expressed at the expression level similar to that of GFP-PAK2-res in the PAK2 siRNA-transfected cells (Fig. 5A). Expression of GFP-PAK2-res, but not GFP-PAK2-res-H82, 85L, restored the proper spindle orientation in the PAK2 siRNA-transfected cells (Fig. 5B), indicating that Cdc42 or Rac1 binding to PAK2 and possibly a subsequent conformational change of PAK2 are required for PAK2 to control the spindle orientation. We investigated the localization of Cdc42 and PAK2 in synchronized HeLa cells. As commercially available antibodies did not work in deter-

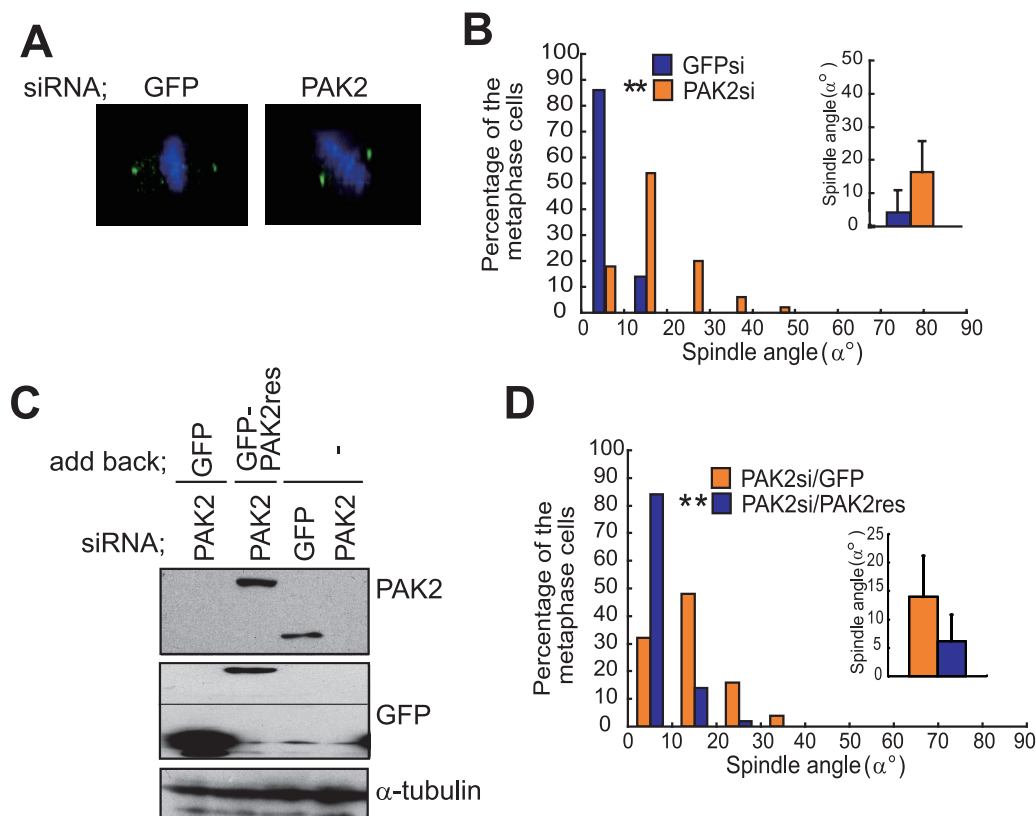


FIG. 4. PAK2 is required for the proper spindle orientation. (A) The X-Z projections of metaphase cells transfected with GFP siRNA or PAK2 siRNA and stained with anti- $\gamma$ -tubulin (green) and Hoechst (blue). (B) Spindle orientation analyses of the cells transfected with the indicated siRNAs. Distribution (histogram;  $n = 50$ ) and the average (inset; mean  $\pm$  standard deviation;  $n = 50$ ) of spindle angles in each condition are shown. \*\*,  $P$  value of  $<0.001$  compared with that of control GFP siRNA, analyzed by F-test. (C) Total lysates of M phase-synchronized cells transfected with GFP siRNA or PAK2 siRNA together with pEGFP or pEGFP-PAK2-res were subjected to immunoblotting with anti-PAK2, anti-GFP, and anti- $\alpha$ -tubulin antibodies. (D) Spindle orientation analysis in the cells transfected with PAK2 siRNA together with pEGFP or pEGFP-PAK2-res. Distribution (histogram;  $n = 50$ ) and the average (inset; mean  $\pm$  standard deviation;  $n = 50$ ) of spindle angles in each condition are shown. \*\*,  $P$  value of  $<0.001$  compared with that of the control pEGFP-transfected cells, analyzed by F-test.

mining the localization of endogenous Cdc42, we investigated the localization of Cdc42 by expressing Myc-tagged Cdc42 (Myc-Cdc42). Both Myc-Cdc42 and endogenous PAK2 were localized to both the cytoplasm and the cortex in metaphase cells (see Fig. S11A and B in the supplemental material). The cortical localization of endogenous PAK2 in metaphase cells was clearly observed in the control GFP siRNA-transfected cells but hardly observed in the PAK2 siRNA-transfected cells (see Fig. S11B in the supplemental material), confirming the cortical localization of PAK2 during metaphase. We further examined subcellular distribution of PAK2 in metaphase cells that were transfected with GFP-siRNA or Cdc42-siRNA. In the GFP siRNA-transfected cells, PAK2 was localized at the cortex (see GFP in Fig. S11C and D in the supplemental material), whereas the cortical localization of PAK2 was mostly lost in the Cdc42-siRNA-transfected cells (see Fig. S11C and D in the supplemental material), suggesting that PAK2 functions downstream from Cdc42 at the cortex in metaphase cells. PAK is a serine/threonine kinase that phosphorylates and regulates the activity of cytoskeletal regulators, including LIM kinase and myosin light chain kinase (3, 38). We investigated whether the kinase activity of PAK2 is required for the spindle orientation control. To this end, we constructed

GFP-PAK2-res-K278R, a GFP fusion of siRNA-resistant, kinase-defective PAK2, in which Lys278 at the ATP binding site was replaced by Arg (45). This kinase-defective form of PAK2 showed an expression level similar to that of GFP-PAK2-res in the PAK2 siRNA-transfected cells (Fig. 5C). Moreover, to our surprise, GFP-PAK2-res-K278R was able to restore the proper spindle orientation in the PAK2 siRNA-transfected cells (Fig. 5D). These results demonstrate that PAK2 regulates spindle orientation in a kinase activity-independent manner.

**PAK2 regulates spindle orientation in a  $\beta$ Pix-dependent manner.** To investigate the kinase-independent function of PAK2 for the control of spindle orientation, we examined the requirement of PAK2-binding proteins for the proper spindle orientation. PAK forms a ternary complex with  $\alpha/\beta$ Pix (36), a guanine nucleotide exchange factor for Rac1 and Cdc42, and Git1/2 (15), a GTPase-activating protein for Arf6. A PAK-Pix-Git complex has been shown to function in various cellular events, including directional chemotaxis of neutrophils, T-cell receptor signaling, cell migration, neurite extension, and centrosome maturation (15, 36, 50). In synchronized HeLa cells, PAK2 bound to  $\beta$ Pix and Git1 during both interphase (0 and 5 h) (Fig. 6A) and M phase (10 h) (Fig. 6A). To investigate the requirement of  $\beta$ Pix or Git1 for the proper spindle orientation,

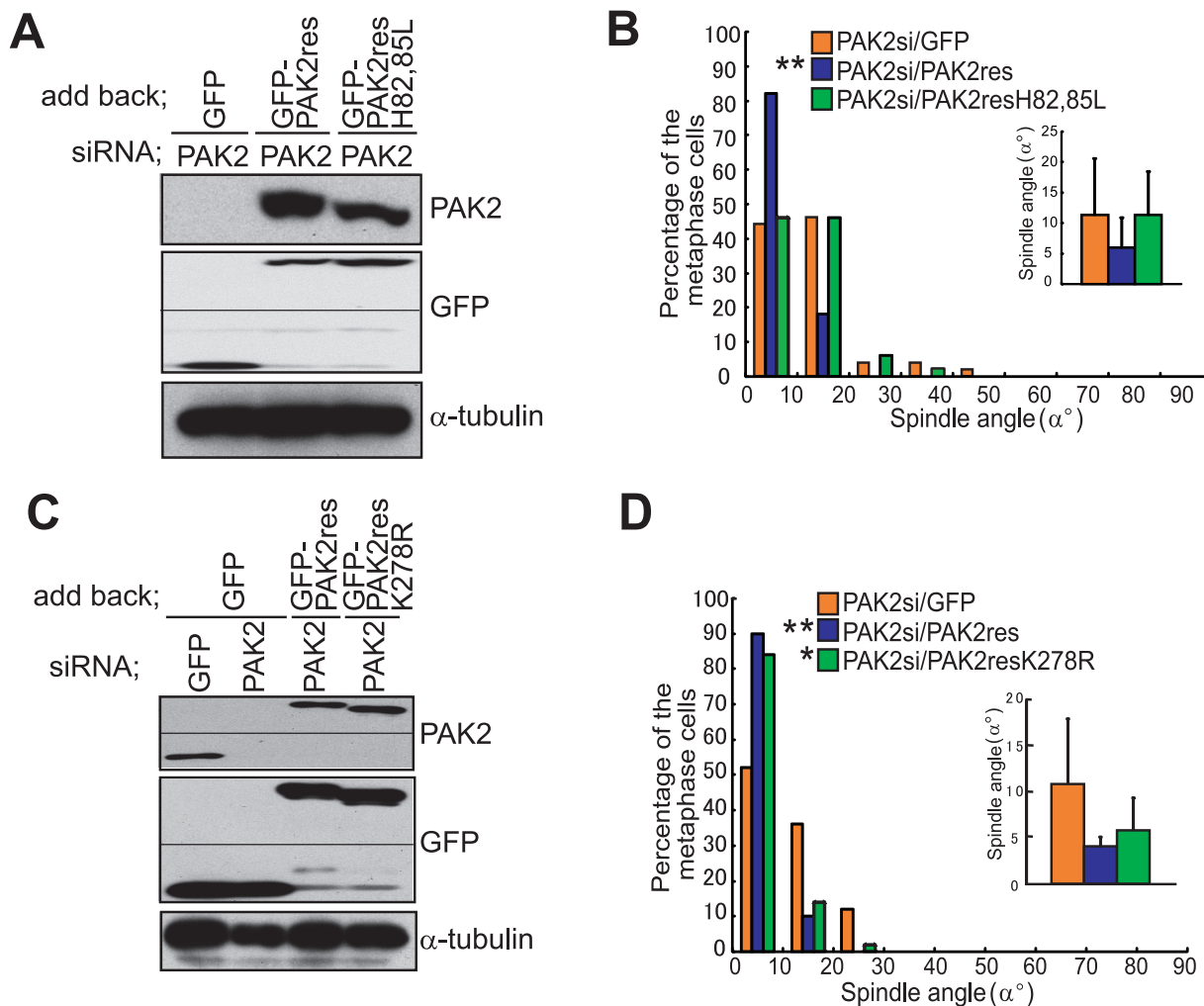


FIG. 5. PAK2 regulates spindle orientation in a Cdc42/Rac1 binding-dependent and kinase activity-independent manner. (A) Total lysates of M phase-synchronized HeLa cells transfected with PAK2 siRNA together with pEGFP, pEGFP-PAK2-res, or pEGFP-PAK2-res-H82, 85L were subjected to immunoblotting with anti-PAK2, anti-GFP, and anti- $\alpha$ -tubulin antibodies. (B) Spindle orientation analysis in the cells transfected with PAK2 siRNA together with pEGFP, pEGFP-PAK2-res, or pEGFP-PAK2-res-H82, 85L. Distribution (histogram;  $n = 50$ ) and the average (inset; mean  $\pm$  standard deviation;  $n = 50$ ) of spindle angles in each condition are shown. \*\*,  $P$  value of  $<0.001$  compared with that of the control pEGFP-transfected cells, analyzed by F-test. (C) Total lysates of M phase-synchronized HeLa cells transfected with GFP siRNA or PAK2 siRNA together with pEGFP, pEGFP-PAK2-res, or pEGFP-PAK2-res-K278R were subjected to immunoblotting with anti-PAK2, anti-GFP, and anti- $\alpha$ -tubulin antibodies. (D) Spindle orientation analysis in the cells transfected with PAK2 siRNA together with pEGFP, pEGFP-PAK2-res, or pEGFP-PAK2-res-K278R. Distribution (histogram;  $n = 50$ ) and the average (inset; mean  $\pm$  standard deviation;  $n = 50$ ) of spindle angles in each condition are shown. \*,  $P$  value of  $<0.01$  and \*\*,  $P$  value of  $<0.001$  compared with those of control pEGFP-transfected cells, analyzed by F-test.

we depleted  $\beta$ Pix or Git1 protein with siRNA in synchronized HeLa cells (Fig. 6B). The spindles were properly oriented in the GFP siRNA- or Git1 siRNA-transfected cells (GFPsi and Git1si) (Fig. 6C) but misoriented in the  $\beta$ Pix siRNA-transfected cells ( $\beta$ Pixsi) (Fig. 6C), indicating that  $\beta$ Pix is required for the spindle orientation control. We next examined whether PAK2 regulates spindle orientation through binding to  $\beta$ Pix. To this end, we constructed Myc-PAK2-res-P185A/R186A, an siRNA-resistant PAK2 mutant, in which Pro185 and Arg186 in the  $\beta$ Pix-binding domain were replaced by Ala, and expressed it in the PAK2 siRNA-transfected cells. This mutant form of PAK2 was reported to be unable to interact with  $\beta$ Pix (39). Myc-PAK2-res-wild-type and Myc-PAK2-res-H82, 85L, but not Myc-PAK2-res-P185A/R186A, interacted with  $\beta$ Pix (Fig.

6D). Myc-PAK2-res-P185A/R186A was expressed at an expression level similar to that of Myc-PAK2-res-wild-type in the PAK2 siRNA-transfected cells (Fig. 6E). Myc-PAK2-res-wild-type, but not Myc-PAK2-res-P185A/R186A, restored the proper spindle orientation (Fig. 6F). These results indicate that  $\beta$ Pix binding to PAK2 is required for PAK2 to control the spindle orientation.

The endogenous PI(3)K activity in M phase-synchronized cells was not significantly changed in the  $\beta$ Pix siRNA-transfected cells (Fig. 6G). However, retraction fibers were reduced, and the cortical actin structures were slightly disrupted in the  $\beta$ Pix siRNA-transfected cells (Fig. 6H). As described above, we have previously shown that these actin structures were essentially normal in the PI(3)K-inhibited cells (43). In addi-

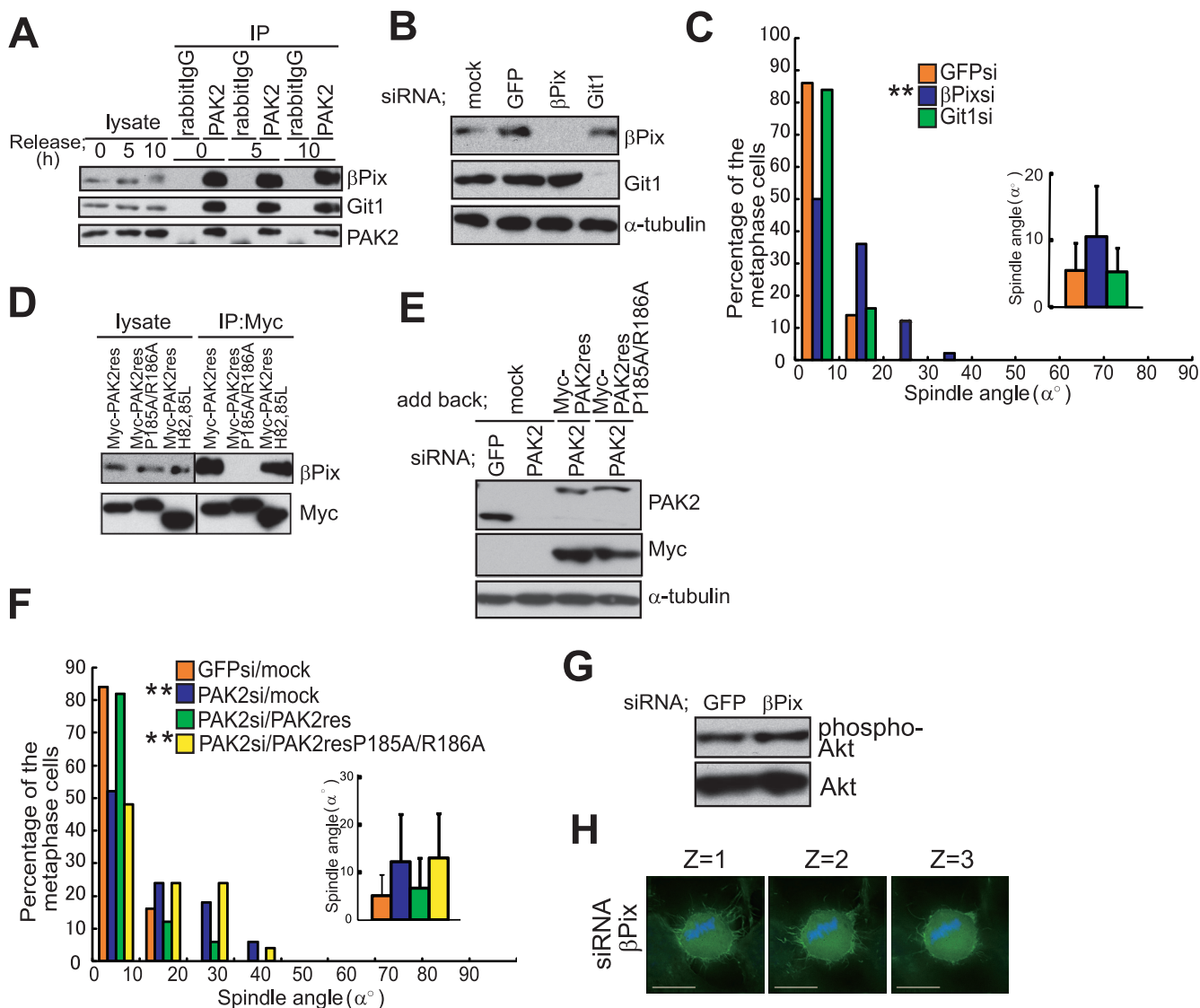


FIG. 6. PAK2 regulates spindle orientation through binding to βPix. (A) Total lysates (80 μl) of synchronized HeLa cells were incubated with anti-PAK2 antibody or rabbit IgG. Total lysates (7.5 μl) and the precipitates were subjected to immunoblotting with anti-βPix, anti-Git1, and anti-PAK2 antibodies. (B) Total lysates of M phase-synchronized HeLa cells transfected with or without (mock) GFP siRNA, βPix siRNA, or Git1 siRNA. GFP siRNA were subjected to immunoblotting with anti-βPix, anti-Git1, and anti-α-tubulin antibodies. (C) Spindle orientation analyses in the cells transfected with GFP siRNA, βPix siRNA, or Git1 siRNA. Distribution (histogram; *n* = 50) and the average (inset; mean ± standard deviation; *n* = 50) of spindle angles in each condition are shown. \*\*, *P* value of <0.001 compared with that of GFP siRNA-transfected cells, analyzed by F-test. (D) Total cell lysates of the cells transfected with pcDL-SRα-myc-PAK2-res, PAK2-res-P185A/R186A, or PAK2-res-H82, 85L were incubated with anti-Myc antibody. The precipitates were subjected to immunoblotting with anti-βPix and anti-Myc antibodies. (E) Total lysates of M phase-synchronized HeLa cells transfected with GFP siRNA or PAK2 siRNA together with or without (mock) pcDL-SRα-myc-PAK2-res or PAK2-res-P185A/R186A were subjected to immunoblotting with anti-PAK2, anti-Myc, and anti-α-tubulin antibodies. (F) Spindle orientation analyses of the cells as prepared in panel E. Distribution (histogram; *n* = 50) and the average (inset; mean ± standard deviation; *n* = 50) of spindle angles in each condition is shown. \*\*, *P* value of <0.001 compared with that of control GFP siRNA-transfected (GFPsi)/mock cells, analyzed by F-test. (G) Total lysates of M phase-synchronized HeLa cells transfected with GFP siRNA or βPix siRNA were subjected to immunoblotting with anti-phospho-Akt (Ser473) and anti-Akt antibodies. (H) Z-stack images (2.5 μm apart) with phalloidin (green) and Hoechst (blue) in metaphase cells transfected with βPix siRNA. The scale bar represents 10 μm.

tion, the interaction between PAK2 and βPix was not significantly changed in the PI(3)K-inhibited cells (see Fig. S12A, B, and C in the supplemental material). These results indicate that a PAK2-βPix module regulates actin reorganization and spindle orientation in a PI(3)K-PtdIns(3,4,5)P3 pathway-independent manner. Moreover, PAK2 depletion in combination with PI(3)K inhibition induced more-severe defects in spindle

orientation than either did alone (see Fig. S13 in the supplemental material). These results, taken together, demonstrate that a PAK2-βPix module and a PI(3)K-PtdIns(3,4,5)P3 pathway act in parallel in the spindle orientation control.

**Cdc42, PAK2, and βPix regulate the distribution of cortical dynein.** We have previously shown that in metaphase cells, dynein/dynactin complexes are accumulated in the midcortex



in a PtdIns(3,4,5)P3-dependent manner, which is important for the proper spindle orientation parallel to the substratum (43). We have found that p150<sup>Glucd</sup>, a subunit of the dynactin complex, is accumulated in the midcortex of the control GFP siRNA-transfected cells (GFP,  $z = 2$  and  $z = 3$ ) (Fig. 7A), consistent with our previous observation (43), but is dispersed in the cortex of the Cdc42 siRNA-, PAK2 siRNA-, and  $\beta$ Pix siRNA-transfected cells (Cdc42, PAK2, and  $\beta$ Pix) (Fig. 7A). The average width for distribution of cortical dynactin along the  $z$  axis fell within 5.8  $\mu$ m in the control cells but is more than 10.0  $\mu$ m, 7.8  $\mu$ m, and 7.1  $\mu$ m in the Cdc42 siRNA-, PAK2 siRNA-, or  $\beta$ Pix siRNA-transfected cells, respectively (Fig. 7B). These results demonstrate that the localized accumulation of dynactin in the midcortex is dependent not only on the PI(3)K-PtdIns(3,4,5)P3 pathway but also on the PAK2- $\beta$ Pix module, both lying downstream from Cdc42.

## DISCUSSION

This study uncovers an essential role of Cdc42 in the control of spindle orientation in adherent cells. We have previously shown that spindles in nonpolarized adherent cells are oriented parallel to the substratum by an actin cytoskeleton- and  $\beta$ 1 integrin-dependent mechanism (42). The spindle misorientation in the cells transfected with both Cdc42 siRNA and  $\beta$ 1 integrin siRNA or in the cells transfected with Cdc42 siRNA and treated with latrunculin B, an actin polymerization inhibitor, is similar to that in the cells transfected with Cdc42 siRNA alone (see Fig. S14 in the supplemental material), suggesting that Cdc42 is a major contributing factor in the  $\beta$ 1 integrin- and actin-dependent mechanism of spindle orientation in HeLa cells. However, it should be noted that spindle orientation is not random but is still largely confined within 50° in the Cdc42-depleted cells (Fig. 1C), as well as in the cells depleted with Cdc42 in combination with the depletion of  $\beta$ 1 integrin or disruption of the actin cytoskeleton (see Fig. S14 in the supplemental material). It should also be noted that depletion of Cdc42 or Rac1, but not RhoA, induces the reduction in the cell area of metaphase cells (see Fig. S6 in the supplemental material). Thus, the geometrical constraints on the spindle orientation in HeLa cells may lower the angles of misoriented spindles. According to the rules of Sachs and Hertwig, the cell's geometrical constraints lay the spindle along the longest axis of the cell (47). The axis of the misoriented spindles observed in Cdc42-depleted cells did not always lie along the longest axis of the cell (data not shown), indicating that cell geometry is not the major contributing factor to spindle orientation in HeLa cells.

Here, we identify two distinct pathways downstream from Cdc42 in this mechanism (Fig. 7C). First, we identify that Cdc42 is required for the activation of PI(3)K during mitosis. Therefore, Cdc42 functions upstream from the PI(3)K-PtdIns(3,4,5)P3 pathway. Cdc42 is also required for PI(3)K activation induced by exogenously added PtdIns(3,4,5)P3 (Fig. 2C). In directed cell migration, such as chemotaxis, a positive feedback loop between Rho family GTPases and PtdIns(3,4,5)P3 is believed to reinforce and establish the PtdIns(3,4,5)P3 polarity and efficient cell migration (29, 44, 46). We have previously proposed that the positive feedback loop functioning at the midcortex amplifies the initial PtdIns(3,4,5)P3

signal to establish and maintain the PtdIns(3,4,5)P3 accumulation in the midcortex during metaphase (43). Therefore, Cdc42 might be involved in the positive feedback loop at the midcortex in metaphase cells. However, our results also show that the activated activity of PI(3)K induced by exogenously added PtdIns(3,4,5)P3 decreased more rapidly in the Cdc42-depleted cells than in control cells (PIP3-histone, Cdc42, and GFP) (Fig. 2D). Thus, it is also possible that Cdc42 negatively regulates PTEN, a lipid phosphatase that dephosphorylates D3 of PtdIns(3,4,5)P3 (26), which we have previously shown to be required for the localized PtdIns(3,4,5)P3 distribution in the midcortex of metaphase cells (43).

Second, our study reveals a novel role of the Cdc42-PAK2/ $\beta$ Pix module in the control of the spindle orientation. Our results also show that PAK1, as well as PAK2, is required for the proper spindle orientation (see Fig. S10 in the supplemental material). The spindle misorientation in the cells transfected with both PAK1- and  $\beta$ Pix siRNA was similar to that in the cells transfected with  $\beta$ Pix siRNA alone (see Fig. S15 in the supplemental material), suggesting that PAK1, as well as PAK2, regulates spindle orientation through  $\beta$ Pix. It should be noted that the defects in the actin cytoskeleton in the Cdc42-depleted cells are more severe than in the cells depleted with PAK2 or  $\beta$ Pix (compare Fig. 3A, D, and H). We speculate that Cdc42 regulates actin remodeling during mitosis through identified PAK2 and  $\beta$ Pix and an unidentified target protein(s), which is important for proper spindle orientation. It should be also noted that the spindle misorientation in the cells transfected with PAK2 siRNA and treated with the PI(3)K inhibitor (see Fig. S13 in the supplemental material) is more severe than in the cells transfected with Cdc42 siRNA (Fig. 1C). We might speculate that transfection of Cdc42 siRNA could not completely downregulate the expression of Cdc42. It would be also possible that other molecules may exist to regulate the PI(3)K-PtdIns(3,4,5)P3 pathway and/or the PAK2- $\beta$ Pix module in the spindle orientation control in a Cdc42-independent manner.

A recent paper has shown that PAK1 is localized to centrosomes and regulates the activation of Aurora A during mitosis (50). Although we could not detect centrosomal localization of endogenous PAK2 with commercially available antibodies, we observed weak signals of GFP-PAK2 in centrosomes of metaphase cells (data not shown). Thus, it would be possible that PAK2 regulates spindle orientation via Aurora A. However, the activation of Aurora A, which could be monitored by the phosphorylation state of Aurora A on Thr288, in the cell extracts from M phase cells (see Fig. S16A in the supplemental material) and its localization at centrosomes in prometaphase cells (see Fig. S16B in the supplemental material) were essentially normal in the PAK2-depleted cells. Therefore, PAK2 seems to regulate spindle orientation in an Aurora A-independent manner. Another paper reported that LIM kinase-mediated cofilin phosphorylation on Ser3 is required for the spindle orientation parallel to the substratum in HeLa cells (19). LIM kinase is known to be phosphorylated and activated by PAK (8). Thus, it would be possible that PAK2 regulates spindle orientation through the LIM kinase-cofilin pathway. However, our results show that the kinase activity of PAK2 is not required for PAK2 to regulate spindle orientation (Fig. 5). Therefore, PAK2 seems to regulate spindle orientation in a LIM kinase-independent manner. Rather,  $\beta$ Pix binding to

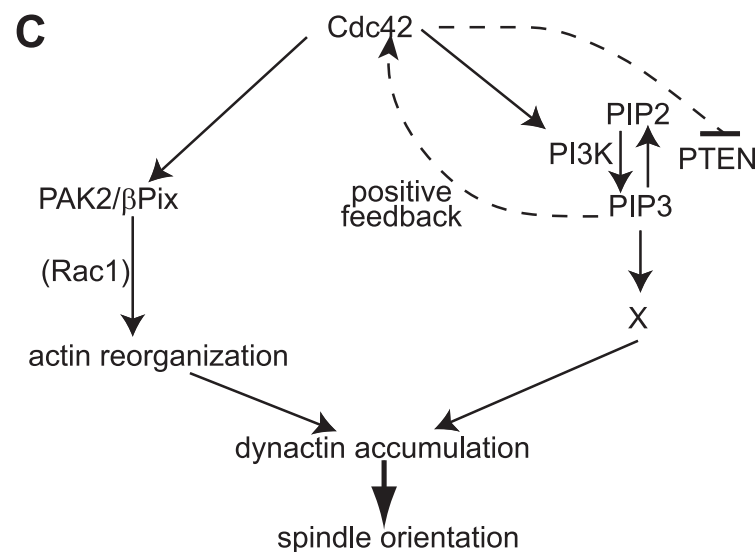
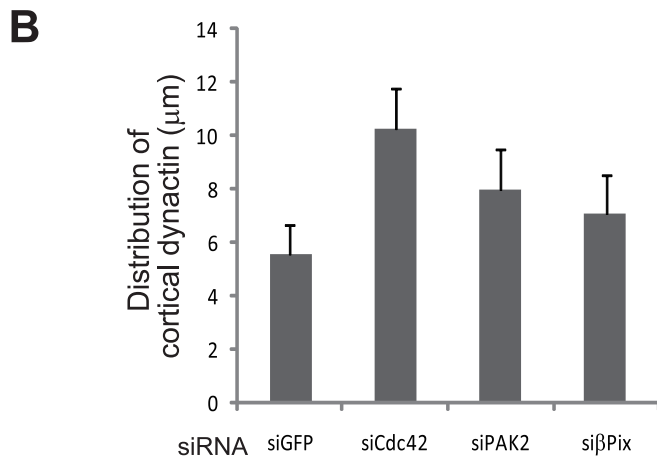
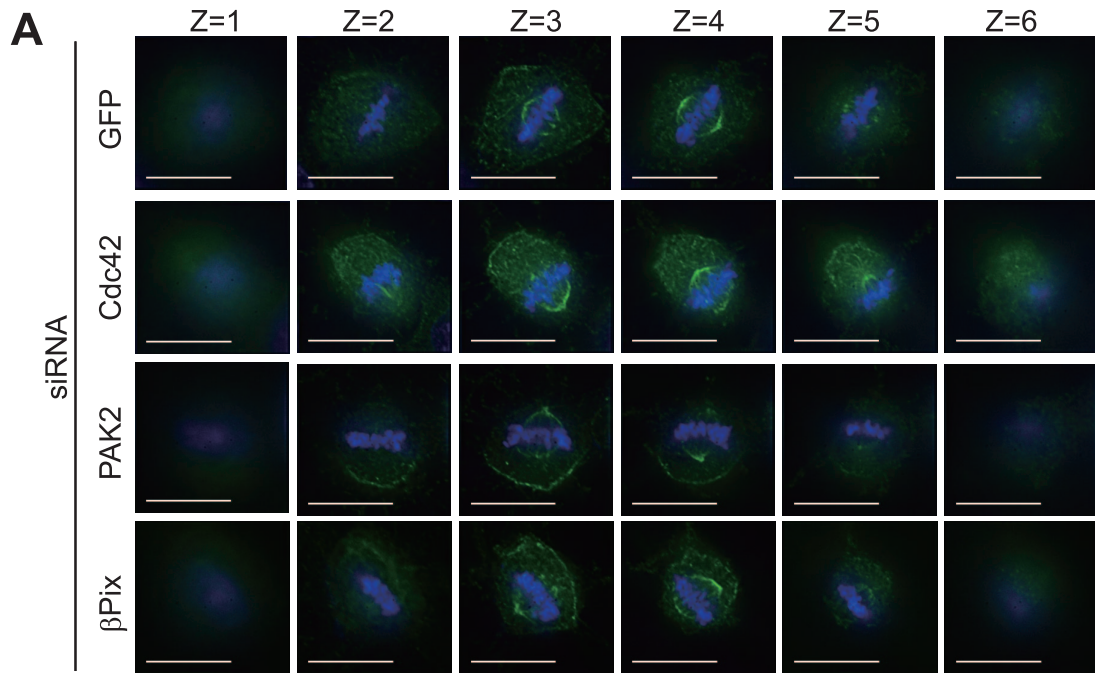


FIG. 7. Cdc42, PAK2, and  $\beta$ Pix regulate the distribution of cortical dynactin. (A) Z-stack images ( $2.5 \mu\text{m}$  apart) with p150<sup>Glued</sup> (green) and Hoechst (blue) in metaphase cells transfected with GFP siRNA, Cdc42 siRNA, PAK2 siRNA, or  $\beta$ Pix siRNA. The scale bar represents  $15 \mu\text{m}$ . (B) Quantification of the widths of distribution for cortical dynactin along the z axis in metaphase cells transfected with the indicated siRNAs. Values are means  $\pm$  standard deviations. ( $n = 20$ ). (C) A model for the two distinct pathways downstream from Cdc42 that control the spindle orientation in nonpolarized adherent cells.

PAK2 is required for PAK2 to control the spindle orientation (Fig. 6). It should be noted that PAK2-res-H82, 85L, which is unable to bind to Cdc42 but able to bind to  $\beta$ Pix, does not restore the proper spindle orientation to the PAK2 siRNA-transfected cells (Fig. 6F). Thus,  $\beta$ Pix binding to PAK2 is not sufficient for the spindle orientation control. We speculate that through binding to Cdc42 or Rac1, PAK2 undergoes a conformational change, and this change may transmit through  $\beta$ Pix to a molecule(s) that is required for the spindle orientation control. It would be possible that PAK2/ $\beta$ Pix complexes regulate actin reorganization and spindle orientation through activating Rac1. Supporting this idea, our results show that the spindle misorientation in the cells transfected with both Rac1 siRNA and Cdc42 siRNA is similar to that in the cells transfected with Cdc42 siRNA alone but is more severe than that in the cells transfected with Rac1 siRNA alone (Fig. 1C), suggesting that Rac1 functions downstream from Cdc42. Our results show that depletion of Git1 by siRNA did not cause spindle misorientation (Fig. 6B and C). Thus, Git1 would be dispensable for the spindle orientation control. However, as HeLa cells express both Git1 and Git2 (10), it is possible that Git2 may compensate for Git1 in the Git1-depleted cells.

We have previously shown that the accumulation of PtdIns(3,4,5)P3 in the midcortex is important for the midcortical localization of dynactin. In this study, we show that actin reorganization by the Cdc42-PAK2/ $\beta$ Pix module is also important for the midcortical localization of dynactin (Fig. 7). It should be noted that midcortical accumulation of dynactin, but not its cortical localization, is disrupted in the Cdc42-, PAK2-, or  $\beta$ Pix-depleted cells (Fig. 7). Thus, the cortical structures required for anchoring dynactin at the cortex are intact in the Cdc42-, PAK2-, or  $\beta$ Pix-depleted cells, but the organizations of cortical structures crucial for accumulating dynactin in the midcortex are disrupted in these cells. Important questions include how the Cdc42-PAK2- $\beta$ Pix module reorganizes cortical structures during mitosis and how this module regulates the dynactin localization and spindle orientation in concert with the PI(3)K-PtdIns(3,4,5)P3 pathway.

While we were preparing this paper, Jaffe et al. reported that Cdc42 regulates spindle orientation in Caco-2 human intestinal epithelial cells cultured in a three-dimensional matrix (17). They found that knockdown of Cdc42 caused spindle misorientation and abnormal cyst formation without affecting the cell polarity. It should be interesting to examine the identified dual pathways downstream from Cdc42 function in the spindle orientation control during epithelial morphogenesis in a three-dimensional culture system.

#### ACKNOWLEDGMENTS

We thank H. Sugimura for providing us with a  $\beta$ Pix-expressing vector.

This work was supported by grants from the Ministry of Education, Culture, Sports, Science and Technology of Japan (E.N.) and PRESTO, JST (F.T.).

#### REFERENCES

- Adams, A. E., D. I. Johnson, R. M. Longnecker, B. F. Sloat, and J. R. Pringle. 1990. CDC42 and CDC43, two additional genes involved in budding and the establishment of cell polarity in the yeast *Saccharomyces cerevisiae*. *J. Cell Biol.* **111**:131–142.
- Balasantil, S., A. A. Sahin, C. J. Barnes, R. A. Wang, R. G. Pestell, R. K. Vadlamudi, and R. Kumar. 2004. p21-activated kinase-1 signaling mediates cyclin D1 expression in mammary epithelial and cancer cells. *J. Biol. Chem.* **279**:1422–1428.
- Bokoch, G. M. 2003. Biology of the p21-activated kinases. *Annu. Rev. Biochem.* **72**:743–781.
- Carminati, J. L., and T. Stearns. 1997. Microtubules orient the mitotic spindle in yeast through dynein-dependent interactions with the cell cortex. *J. Cell Biol.* **138**:629–641.
- Chan, A. Y., S. J. Coniglio, Y. Y. Chuang, D. Michaelson, U. G. Knaus, M. R. Philips, and M. Symons. 2005. Roles of the Rac1 and Rac3 GTPases in human tumor cell invasion. *Oncogene* **24**:7821–7829.
- Cowan, C. R., and A. A. Hyman. 2004. Asymmetric cell division in *C. elegans*: cortical polarity and spindle positioning. *Annu. Rev. Cell Dev. Biol.* **20**:427–453.
- Deroanne, C. F., D. Hamelryckx, T. T. Ho, C. A. Lambert, P. Catroux, C. M. Lapierre, and B. V. Nussgens. 2005. Cdc42 downregulates MMP-1 expression by inhibiting the ERK1/2 pathway. *J. Cell Sci.* **118**:1173–1183.
- Edwards, D. C., L. C. Sanders, G. M. Bokoch, and G. N. Gill. 1999. Activation of LIM-kinase by Pak1 couples Rac/Cdc42 GTPase signaling to actin cytoskeletal dynamics. *Nat. Cell Biol.* **1**:253–259.
- Etienne-Manneville, S., and A. Hall. 2002. Rho GTPases in cell biology. *Nature* **420**:629–635.
- Frank, S. R., M. R. Adelstein, and S. H. Hansen. 2006. GIT2 represses Crk- and Rac1-regulated cell spreading and Cdc42-mediated focal adhesion turnover. *EMBO J.* **25**:1848–1859.
- Glotzer, M. 2001. Animal cell cytokinesis. *Annu. Rev. Cell Dev. Biol.* **17**:351–386.
- Gonczy, P., S. Pichler, M. Kirkham, and A. A. Hyman. 1999. Cytoplasmic dynein is required for distinct aspects of MTOC positioning, including centrosome separation, in the one cell stage *Caenorhabditis elegans* embryo. *J. Cell Biol.* **147**:135–150.
- Gotta, M., M. C. Abraham, and J. Ahringer. 2001. CDC-42 controls early cell polarity and spindle orientation in *C. elegans*. *Curr. Biol.* **11**:482–488.
- Haller, C., S. Rauch, N. Michel, S. Hannemann, M. J. Lehmann, O. T. Keppler, and O. T. Fackler. 2006. The HIV-1 pathogenicity factor Nef interferes with maturation of stimulatory T-lymphocyte contacts by modulation of N-Wasp activity. *J. Biol. Chem.* **281**:19618–19630.
- Hoefen, R. J., and B. C. Berk. 2006. The multifunctional GIT family of proteins. *J. Cell Sci.* **119**:1469–1475.
- Hoffman, D. B., C. G. Pearson, T. J. Yen, B. J. Howell, and E. D. Salmon. 2001. Microtubule-dependent changes in assembly of microtubule motor proteins and mitotic spindle checkpoint proteins at PtK1 kinetochores. *Mol. Cell Biol.* **21**:1995–2009.
- Jaffe, A. B., N. Kaji, J. Durgan, and A. Hall. 2008. Cdc42 controls spindle orientation to position the apical surface during epithelial morphogenesis. *J. Cell Biol.* **183**:625–633.
- Jaffe, A. B., and A. Hall. 2005. Rho GTPases: biochemistry and biology. *Annu. Rev. Cell Dev. Biol.* **21**:247–269.
- Kaji, N., A. Muramoto, and K. Mizuno. 2008. LIM-kinase-mediated cofilin phosphorylation during mitosis is required for precise spindle positioning. *J. Biol. Chem.* **283**:4983–4992.
- Le Borgne, R., Y. Bellaiche, and F. Schweisguth. 2002. Drosophila E-cadherin regulates the orientation of asymmetric cell division in the sensory organ lineage. *Curr. Biol.* **12**:95–104.
- Lei, M., W. Lu, W. Meng, M. C. Parrini, M. J. Eck, B. J. Mayer, and S. C. Harrison. 2000. Structure of PAK1 in an autoinhibited conformation reveals a multistage activation switch. *Cell* **102**:387–397.
- Lu, B., F. Roegiers, L. Y. Jan, and Y. N. Jan. 2001. Adherens junctions inhibit asymmetric division in the *Drosophila* epithelium. *Nature* **409**:522–525.
- Ma, C., H. A. Benink, D. Cheng, V. Montplaisir, L. Wang, Y. Xi, P. P. Zheng, W. M. Bement, and X. J. Liu. 2006. Cdc42 activation couples spindle positioning to first polar body formation in oocyte maturation. *Curr. Biol.* **16**:214–220.
- Macara, I. G. 2004. Parsing the polarity code. *Nat. Rev. Mol. Cell Biol.* **5**:220–231.
- Maddox, A. S., and K. Burridge. 2003. RhoA is required for cortical retraction and rigidity during mitotic cell rounding. *J. Cell Biol.* **160**:255–265.
- Maehama, T., and J. E. Dixon. 1998. The tumor suppressor, PTEN/MMAC1, dephosphorylates the lipid second messenger, phosphatidylinositol 3,4,5-trisphosphate. *J. Biol. Chem.* **273**:13375–13378.
- Mitchison, T. J. 1992. Actin based motility on retraction fibers in mitotic PtK2 cells. *Cell Motil. Cytoskeleton* **22**:135–151.
- Na, J., and M. Zernicka-Goetz. 2006. Asymmetric positioning and organization of the meiotic spindle of mouse oocytes requires CDC42 function. *Curr. Biol.* **16**:1249–1254.
- Niggli, V. 2005. Regulation of protein activities by phosphoinositide phosphates. *Annu. Rev. Cell Dev. Biol.* **21**:57–79.
- O'Connell, C. B., and Y. L. Wang. 2000. Mammalian spindle orientation and position respond to changes in cell shape in a dynein-dependent fashion. *Mol. Biol. Cell* **11**:1765–1774.
- Pearson, C. G., and K. Bloom. 2004. Dynamic microtubules lead the way for spindle positioning. *Nat. Rev. Mol. Cell Biol.* **5**:481–492.

32. **Rappaport, R.** 1996. Cytokinesis in animal cells. Cambridge University Press, Cambridge, United Kingdom.
33. **Ridley, A. J.** 2006. Rho GTPases and actin dynamics in membrane protrusions and vesicle trafficking. *Trends Cell Biol.* **16**:522–529.
34. **Roberts, E. C., P. S. Shapiro, T. S. Nahreini, G. Pages, J. Pouyssegur, and N. G. Ahn.** 2002. Distinct cell cycle timing requirements for extracellular signal-regulated kinase and phosphoinositide 3-kinase signaling pathways in somatic cell mitosis. *Mol. Cell. Biol.* **22**:7226–7241.
35. **Roegiers, F., and Y. N. Jan.** 2004. Asymmetric cell division. *Curr. Opin. Cell Biol.* **16**:195–205.
36. **Rosenberger, G., and K. Kutsche.** 2006. AlphaPIX and betaPIX and their role in focal adhesion formation. *Eur. J. Cell Biol.* **85**:265–274.
37. **Sells, M. A., U. G. Knaus, S. Bagrodia, D. M. Ambrose, G. M. Bokoch, and J. Chernoff.** 1997. Human p21-activated kinase (Pak1) regulates actin organization in mammalian cells. *Curr. Biol.* **7**:202–210.
38. **Sells, M. A., and J. Chernoff.** 1997. Emerging from the Pak: the p21-activated protein kinase family. *Trends Cell Biol.* **6**:162–167.
39. **Shin, E., K. Shin, C. Lee, K. Woo, S. Quan, N. Soung, Y. G. Kim, C. I. Cha, S. Kim, D. Park, G. M. Bokoch, and E. Kim.** 2002. Phosphorylation of p85  $\beta$ Pix, a Rac/Cdc42-specific guanine nucleotide exchange factor, via the Ras/ERK/PAK2 pathway is required for basic fibroblast growth factor-induced neurite outgrowth. *J. Biol. Chem.* **277**:44417–44430.
40. **Shtivelman, E., J. Sussman, and D. Stokoe.** 2002. A role for PI 3-kinase and PKB activity in the G2/M phase of cell cycle. *Curr. Biol.* **12**:919–924.
41. **Takai, Y., T. Sasaki, and T. Matozaki.** 2001. Small GTP-binding proteins. *Physiol. Rev.* **81**:153–208.
42. **Toyoshima, F., and E. Nishida.** 2007. Integrin-mediated adhesion orients the spindle parallel to the substratum in an EB1- and myosin X-dependent manner. *EMBO J.* **26**:1487–1498.
43. **Toyoshima, F., S. Matsumura, H. Morimoto, M. Mitsushima, and E. Nishida.** 2007. PtdIns(3,4,5)P3 regulates spindle orientation in adherent cells. *Dev. Cell* **13**:796–811.
44. **Van Haastert, P. J., and P. N. Devreotes.** 2004. Chemotaxis: signaling the way forward. *Nat. Rev. Mol. Cell Biol.* **8**:626–634.
45. **Walter, B. N., Z. Huang, R. Jakobi, P. T. Tuazon, E. S. Alnemri, G. Litwack, and J. A. Traugh.** 1998. Cleavage and activation of p21-activated protein kinase gamma-PAK by CPP32 (caspase 3). Effects of autophosphorylation on activity. *J. Biol. Chem.* **273**:28733–28739.
46. **Weiner, O. D., P. O. Neilsen, G. D. Prestwich, M. W. Kirschner, L. C. Cantley, and H. R. Bourne.** 2002. A PtdInsP(3)- and Rho GTPase-mediated positive feedback loop regulates neutrophil polarity. *Nat. Cell Biol.* **4**:509–513.
47. **Wilson, E. B.** 1925. The cell in development and heredity, 3rd ed. The Macmillan Company, New York, NY.
48. **Yamashita, Y. M., D. L. Jones, and M. T. Fuller.** 2003. Orientation of asymmetric stem cell division by the APC tumor suppressor and centrosome. *Science* **301**:1547–1550.
49. **Yasuda, S., F. Oceguera-Yanez, T. Kato, M. Okamoto, S. Yonemura, Y. Terada, T. Ishizaki, and S. Narumiya.** 2004. Cdc42 and mDia3 regulate microtubule attachment to kinetochores. *Nature* **428**:767–771.
50. **Zhao, Z. S., J. P. Lim, Y. W. Ng, L. Lim, and E. Manser.** 2005. The GIT-associated kinase PAK targets to the centrosome and regulates Aurora-A. *Mol. Cell* **20**:237–249.